

The temporal properties of the response of macaque ganglion cells and central mechanisms of flicker detection

Barry B. Lee

SUNY College of Optometry, New York, USA, &
Max Planck Institute for Biophysical Chemistry,
Göttingen, Germany



Hao Sun

Buskerud University College, Kongserg, Norway, &
SUNY College of Optometry, New York, USA



Walter Zucchini

Institute for Statistics and Econometrics,
University of Göttingen, Germany



This analysis assesses sensitivity of primate ganglion cells to sinusoidal modulation as a function of temporal frequency, based on the structure of their impulse trains; sensitivity to luminance and chromatic modulation was compared to human psychophysical sensitivity to similar stimuli. Each stimulus cycle was Fourier analyzed, and response amplitudes subjected to neurometric analysis; this assumes a detector with duration inversely proportional to frequency, that is, the stimulus epoch analyzed is a single cycle rather than a fixed duration, and provides an upper bound for a detection by an observer who bases judgments on a single cell. Signal-to-noise ratio for a given Fourier amplitude rapidly decreased with temporal frequency. This is a consequence of the statistics of impulse trains making up the response; at higher temporal frequencies, there are fewer impulses per cycle. Performance of this “single-cell” observer was then compared with that of modeled central detection mechanisms of fixed duration. For chromatic modulation, a filter/detector with a time constant of ~40 ms operating upon the parvocellular (PC) pathway provided a match to psychophysical results, whereas for luminance modulation, a filter/detection mechanism operating upon the magnocellular (MC) pathway with a time constant of ~5–10 ms provided a suitable match. The effects of summation and nonlinear interactions between cell inputs to detection are also considered in terms of enhanced sensitivity and “sharpness” of thresholds, that is, the steepness of the neurometric function. For both luminance (MC cells) and chromatic modulation (PC cells), restricted convergence (<20 cells) appears adequate to provide sharp thresholds and sensitivity comparable to psychophysical performance.

Keywords: parvocellular, magnocellular, flicker, luminance, chromatic, neurometric

Citation: Lee, B. B., Sun, H., & Zucchini, W. (2007). The temporal properties of the response of macaque ganglion cells and central mechanisms of flicker detection. *Journal of Vision*, 7(14):1, 1–16, <http://journalofvision.org/7/14/1/>, doi:10.1167/7.14.1.

Introduction

We have previously described the temporal response (modulation transfer function; MTF) of ganglion cells of the parvocellular (PC) and magnocellular (MC) pathways to luminance and chromatic modulation and then compared the results with human psychophysical performance (Lee, Pokorny, Smith, Martin, & Valberg, 1990). The analysis was generally consistent with MC cells being the substrate for detection of luminance modulation and PC cells acting as a substrate for detection of red–green chromatic modulation, except that cell responses persisted to higher temporal frequencies than did psychophysical sensitivity. This was particularly marked for PC cells with chromatic modulation; cells responded up to 30–40 Hz, compared to a psychophysical fusion limit of 10–15 Hz. We postulated central, temporal low-pass filters operating on cell signals to account for these discrepancies.

In a recent study (Sun, Rüttiger, & Lee, 2004), we measured signal-to-noise ratio of responses to drifting gratings and found that, for a given Fourier amplitude, signal-to-noise ratio rapidly decreased with temporal frequency but was largely independent of spatial frequency and contrast. This was shown to be due to the nature of the response as an impulse train. As frequency increases (i.e., cycle duration decreases), so does the number of impulses per cycle; also timing variability inherent in impulse generation plays a relatively larger role. Both these factors will decrease signal-to-noise ratio. Responses modeled on the basis of a modulated Poisson process showed similar features. We would stress that we have no evidence that there is an increase in inherent noise in the response as temporal frequency increases; the effect observed appears to be solely a consequence of the structure of the impulse train.

In relating psychophysical sensitivity to cell responses, signal-to-noise ratio of cell signals must be taken into

account. We here reassess temporal MTFs for single cells by performing a neurometric analysis of responses, that is, by applying an “ideal observer” analysis to response spike trains. This provides an upper bound to sensitivity of an observer who bases detection on a single ganglion cell. We term this individual the “single-cell observer.” Such an analysis, however, assumes a detector that changes its time constant inversely with temporal frequency.

Actual psychophysical detection of luminance and chromatic modulation must depend on the characteristics of central detection mechanisms and on cellular convergence upon them. For example, the critical duration for chromatic detection is several times longer than that for luminance detection (200–300 vs. 50–100 ms), and this can be directly related to luminance and chromatic MTFs (Swanson, Ueno, Smith, & Pokorny, 1987). The difference presumably reflects different time constants of different detection mechanisms. The single-cell observer analysis provides a context in which models of central detection mechanisms can be assessed. By comparing psychophysical performance with the behavior of such models using ganglion cell spike trains as input, one might hope to constrain model properties.

A satisfactory model should meet several criteria. It should yield the psychophysical MTF and should achieve the absolute sensitivity of real, human observers. Psychophysical sensitivity greater than expected of the single cell could occur through summation of some kind, either by convergence of many cells into one detector or by probability summation (Watson, 1979). A further issue concerns the steepness of the detection curve, that is, of the relation between the observer’s percentage correct responses and contrast in, for example, a two-alternative forced choice paradigm. Such curves are usually fitted with a Weibull function. In a seminal study, Tolhurst, Movshon, and Dean (1983) considered noise in spike trains of cortical cells. They pointed out that neurometric curves, which relate percent correct to stimulus contrast based on a single cell, are fit by Weibull functions of much shallower slope (typically with a slope parameter of 1.5–2) than is generally the case for psychophysical data (slope parameters 3–5). They proposed that probability multiplication (a response only when several detectors are activated) would steepen neurometric slopes, at the cost of some decrease of sensitivity. They suggested that, by a combination of probability summation and multiplication, the cortex could increase both sensitivity and function slope. This is a feasible strategy for cortex where cell numbers are large, but, for a psychophysical stimulus of given size, convergence among ganglion cell inputs onto a detector is constrained by ganglion cell density. The issue is complex, especially when common noise in detector inputs is considered. Britten, Newsome, Shadlen, Celebrini, and Movshon (1996) have explored this issue with regard to MT neurons.

We consider here the characteristics of central detection mechanisms responsible for detection of sinusoidal

modulation. We compare performance of models of central detection with that of a single-cell observer, and we consider how factors such as summation of inputs, or other kinds of operation, may influence their properties. This is a first step; a complete model would have to take the spatial factors into account, and these have complex effects on flicker detection. Some of these issues are raised in the discussion.

Methods

Cell activity was recorded from the retinas of anesthetized macaques (*Macaca fascicularis*). The animals were initially sedated with an intramuscular injection of ketamine (10 mg/kg) followed by thiopental (10 mg/kg). Anesthesia was maintained with inhaled isoflurane (0.2–2%) in a 70:30 N₂O–O₂ mixture. Local anesthetic was applied to points of surgical intervention. EEG and ECG were continuously monitored to ensure animal health and adequate depth of anesthesia. Muscle relaxation was maintained by a constant infusion of gallamine triethiodide (5 mg/kg/hr iv) with accompanying dextrose Ringer solution (6 ml/kg/hr). Body temperature was kept close to 37.5°. End tidal CO₂ was adjusted to close to 4% by adjusting the rate of respiration. All procedures were approved by the SUNY Animal Care Committee and conform to ARVO guidelines for ethical care of animals.

Neuronal activity was directly recorded from retinal ganglion cells by a tungsten-in-glass electrode inserted through a cannula entering the eye behind the limbus. Optimal tip exposure was 4–5 μ m for MC cells and 2–3 μ m for PC cells, with resistances of 20–60 M Ω . The details of the preparation can be found elsewhere (Crook, Lange-Malecki, Lee, & Valberg, 1988). We recorded responses of cells between 4° and 12° eccentricity (PC cells mean 6.7°, MC cells mean 8.4°). Cell identification was achieved through standard tests (Lee, Martin, & Valberg, 1989). These included achromatic contrast sensitivity and responses to lights of different chromaticity. Additional tests, for example, measuring responses to heterochromatically modulated lights (Smith, Lee, Pokorny, Martin, & Valberg, 1992), were employed in cases when identification was difficult. PC cells can generally be identified by their tonic responses and spectral opponency, and MC cells can be identified by their phasic responses and lack of spectral opponency. For each cell, the locus of the receptive field center was determined and the stimulus was centered on this point. Times of spike occurrence were recorded to an accuracy of 0.1 ms, and averaged histograms of spike trains were simultaneously accumulated with 64 bins per cycle of modulation.

Visual stimuli were generated using a light emitting diode (LED) based Maxwellian view system (Pokorny, Smithson, & Quinlan, 2004). Only two LED sources were used in these experiments, and they had peak wavelengths

of 518 and 660 nm, with half-height bandwidths of 8–10 nm. A few measurements were used which were obtained using a similar, earlier system (Lee et al., 1990) with LED sources with dominant wavelengths of 554 and 638 nm. The chromaticity of each LED and their relative luminance were calculated from each LED's spectrum and the Smith and Pokorny (1972) cone fundamentals. Mean LED outputs were adjusted such that the two LEDs provided the same luminance. Absolute mean retinal illuminance (2,000 td; this is equivalent to ~2,800 td for the monkey retina due to the smaller eye size; Virsu & Lee, 1983) was estimated as in Westheimer (1966). LEDs were sinusoidally modulated with a frequency-modulated constant-amplitude pulse train (100 kHz) at frequencies from 0.61 to 78 Hz and at a variety of contrasts (8–13 per stimulus condition). Dependent upon temporal frequency, 30–200 cycles were accumulated per condition. In one set of experiments, rectangular 1,500-ms chromatic pulses of different contrasts were delivered, either in a redward (+L–M cells) or greenward (+M–L cells) direction. Interpulse interval was 4,500 ms, and 30 pulses were delivered at each contrast. The stimulus field was 4.7° in diameter, centered on the receptive field and with a dark surround.

Analysis of physiological data

MC and PC cells were selected for analysis based on long-term stability of recording, completeness of data sets, and responsivities falling within the typical range for the cells concerned. Cells chosen showed little or no drifts of maintained activity or responsivity (which are rare in retina), and several seconds rest was imposed between stimulus conditions. Cell responses analyzed in detail were at least 5 per cell class, and these cells were typical of a larger data sample from which incomplete data sets were obtained. Analysis methods are described in a later section; they generated the data shown in Figures 1–8.

For analyses in which input of multiple cells to a detection mechanism were considered, we required up to 16 cells with similar maintained activity, and the physiological database was inadequate. We therefore simulated cell response spike trains using Monte Carlo methods using the following steps: (1) For a given frequency and contrast, a response template was constructed, either from the lower harmonics (0–9) of Fourier spectrum or from the smoothed response histogram of several cells. (2) This template provided a measure of the probability of impulse occurrence at each point within a stimulus cycle, $P(t)$. We developed an algorithm that generated artificial impulse trains that closely matched real measurements in their interval statistics (B. B. Lee and H. Sun, in preparation). Briefly, the method is based on a renewal process with a dead time randomly drawn from a Gaussian distribution, the mean and the standard

deviation of which were proportional to $P(t)$. This principle has been used to simulate impulse distributions in maintained activity (Teich, Matin, & Cantor, 1978).

Results

Principles of data analysis

We first describe characteristics of responses to individual cycles of modulation. This analysis is then used in the development of the single-cell observer.

We take as example responses of M, L-cone opponent PC cells to chromatic modulation. The impulse train to each cycle of modulation was Fourier analyzed to give real and imaginary response components. An example is plotted in Figure 1A, where each point represents the response to a single cycle. The points can be seen to form a radially symmetric cluster; the mean vector is also shown. Between-cycle variation was termed noise by Croner, Purpura, and Kaplan (1993) and defined as

$$\text{Noise} = \sqrt{\frac{\sum_1^n d_i^2}{n-1}}. \quad (1)$$

As shown earlier for achromatic gratings (Sun et al., 2004), this noise measure rapidly increased with modulation frequency but was usually independent of contrast. This is illustrated in Figures 1B–1D. Figure 1B shows the Fourier response components at three selected frequencies. The scatter of single-cycle response amplitudes substantially increases from 0.61 to 19.8 Hz (50% contrast data are shown), although the mean vector length (line segments) increases only moderately. This relationship is plotted in Figure 1C, averaged over five cells. Variability increases more rapidly than response amplitude and exceeds the latter at 40 Hz. Thus, for a given Fourier amplitude, signal-to-noise ratio decreases with temporal frequency. The results shown here with chromatic modulation and PC cells are similar to those with achromatic gratings in Sun et al., in which we showed that the increase in variability with frequency is a consequence of the statistics of impulse trains. As in the earlier work, when response amplitude increased with contrast, the noise measure remains stable (Figure 1D; 4.88 Hz data shown). The response values have been fitted with a Naka–Rushton function (Naka & Rushton, 1966). The initial slope of this function provides an estimate of contrast gain.

In the earlier study on ganglion cell temporal responsiveness (Lee et al., 1990), we used the fitted Naka–Rushton functions to estimate the contrast required for a 20 impulse per second (imp/s) modulation in firing. However, this did not consider the substantial increase in response

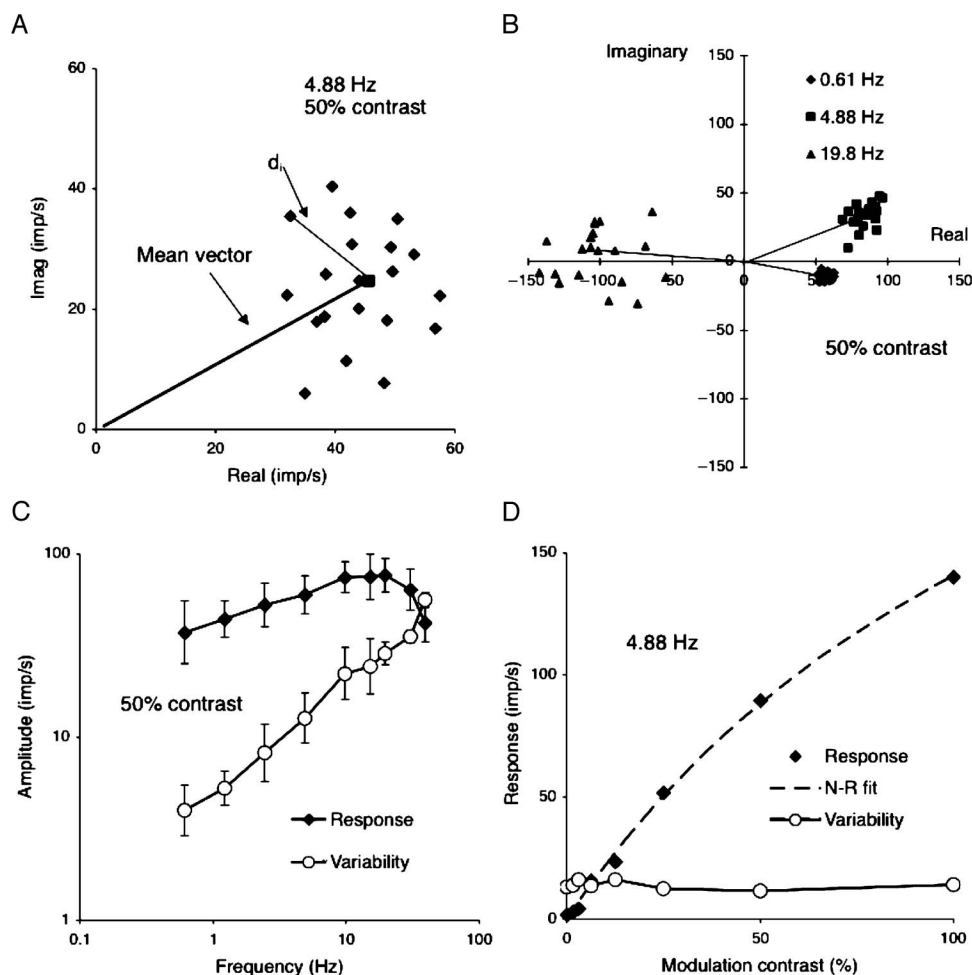


Figure 1. Basics of response analysis. (A) Each point represents real and imaginary components from the Fourier analysis of one cycle of response of a +L–M parvocellular (PC) cell to chromatic modulation at 4.88 Hz, 50% contrast. The square shows the mean response and the mean vector is drawn in. d_i is the distance between each point and mean and is used to calculate noise as described in the text. (B) Responses of a +L–M PC cells at three temporal frequencies; 50% modulation. Individual cycles and mean vectors are shown. The scatter increases substantially with temporal frequency although length of the response vector increases only moderately. The mean vector rotates due to response latency. (C) Response amplitude (signal) and variability (noise) as a function of temporal frequency. Mean of five PC cells, both +M–L and +L–M cells combined, 50% modulation. Variability increases more steeply with temporal frequency than does amplitude, resulting in a decrease in signal-to-noise ratio. (D) Response amplitude and variability for a +L–M PC cell as a function of contrast at 4.88 Hz. Response amplitude increases with contrast but variability remains constant. Responses have been fitted by a Naka–Rushton function.

variability with temporal frequency. We now describe the single-cell observer approach that takes this into account.

We performed a neurometric analysis based on first-harmonic Fourier amplitudes. Figure 2A shows results of a single-cycle Fourier analysis for 4.88 Hz chromatic modulation at 0% and 6.25% contrast; only a subset of data are shown for clarity. The 0% points cluster around zero, and the low-contrast responses form a cluster displaced away from the origin, each point with a response vector amplitude, R_i . To perform the neurometric analysis, the response vector amplitudes were each expressed as a Gaussian and then summed over all cycles, as shown in Figure 2B; the smoothing Gaussian is shown in the inset. Absolute response vector is plotted on the

abscissa and percentage of trials on the ordinate. The two distributions show some overlap.

Instead of using absolute response amplitude, one can take the response vector amplitude at the mean response phase, that is, the projection of each response vector onto the mean response vector ($R_{i\text{phase}}$). The mean response vector is shown as the dashed line in Figure 2A. This would be equivalent to the observer or the detection mechanism knowing the phase of response. With a continuous sinusoidal stimulus, this would not be the case, but if, for example, an observer was presented with a single stimulus with a cue, then stimulus timing would be known. This alternative analysis thus gives an estimate of the effect of removing timing uncertainty. Knowing

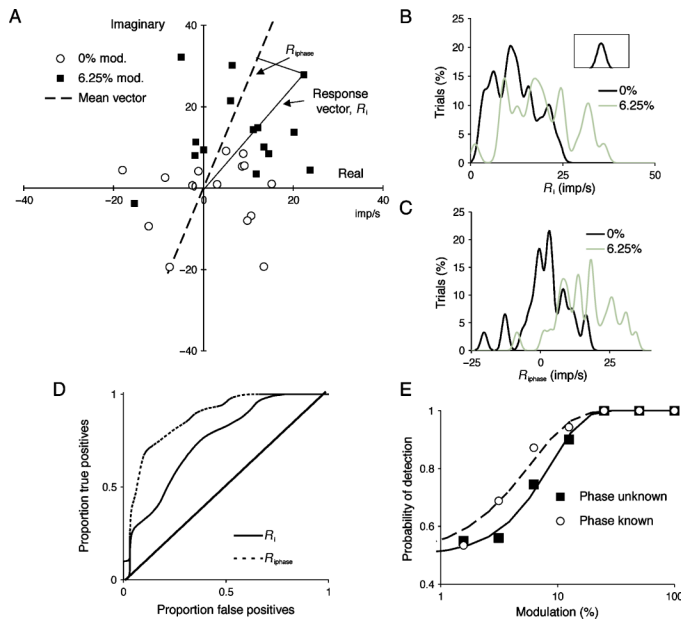


Figure 2. Single-cell observer analysis. (A) Responses of +L–M parvocellular (PC) cell to 4.88 Hz chromatic modulation, at 0% and 6.25% contrast. Responses at 0% contrast cluster around zero, at 6.25% they are displaced from zero with some overlap. For each response, the vector R_i was used in subsequent analysis. Alternatively, the response component along the mean vector ($R_{i\text{phase}}$) was used. Only a subset of the 30 cycles recorded for each contrast is shown for clarity. (B, C) Amplitude values were cumulated after smoothing with the inset Gaussian. The cumulative distributions for all sweeps are shown for the two contrasts (0% and 6.25%). (D) The cumulative proportion of signal plotted relative to noise as the response measures (R_i or $R_{i\text{phase}}$) increase for a given contrast (in this case 6.25%) provides an receiver operating characteristic (ROC) curve. The abscissa represents proportion of false-positives (false alarms) and the ordinate true positives (hits). The diagonal indicates a contrast of zero. (E) The area under curves as in panel D gives the percent correct of detection based on a single cell in a two-alternative forced choice situation. This is plotted against contrast and was fitted with a Weibull function using maximum likelihood estimation. The curve for the known phase condition is shifted leftward compared to the unknown phase condition, indicating that knowing response phase increases detectability.

response phase (or timing) would be expected to improve detection. The summed distribution of vector amplitudes shows greater separation (Figure 2C) and subsequent figures show there is some improvement in detectability.

Amplitude distributions (Figures 2B and 2C) can be used to generate receiver operating characteristic (ROC) curves (Lee, Wehrhahn, Westheimer, & Kremers, 1993), as shown in Figure 2D, by cumulating the amplitude distributions for signal and noise. The approach is equivalent to a two-alternative forced choice procedure, in which one interval contains a stimulus of given contrast and the other contains no modulation. The area under the

ROC curve can be summed to give the probability of detection based on a single cell, which is plotted as a function of contrast in Figure 2E. The data have been fitted by Weibull functions using maximum likelihood estimation (Watson, 1979). Detection threshold in the known phase case is lower (curve shifted leftward) than when the phase is unknown. The slopes in the examples shown are 1.62 and 1.24, which is typical for single cell neurometric analyses (Tolhurst et al., 1983). From analyses such as that in Figure 2, single-cell thresholds for 75% correct detection were calculated as a function of temporal frequency.

Our analysis of detectability based on first-harmonic thresholds assumes that there is little response energy in higher harmonics. This was generally the case at low contrasts. At a 10 imp/s first-response amplitude, there was on average 7.9 times more energy in the first than the second harmonic (averaged over five PC cells, each at nine frequencies). In addition, first-harmonic phase varied little with contrast at firing rates greater than 5 imp/s but second-harmonic phases were more variable. This would indicate a lack of useful information for detection.

Figures 1 and 2 represent a neurometric analysis in which neural responses are compared to maintained activity. It does not assume a detection mechanism with, for example, a specific time constant, and it provides the maximum sensitivity that can be attained by a detector based on a single cell, that is, the single-cell observer.

Temporal sensitivity of PC and MC single-cell observers

We now consider the temporal sensitivity of MC and PC cells derived as in the previous section. The analysis in Figure 2 was performed at a range of temporal frequencies, and Figure 3A shows averaged sensitivities for PC cells and red–green chromatic modulation ($n = 5$). Data for +L–M and +M–L cells were similar and have been combined. Cone contrast (mean of M and L) was calculated using the cone fundamentals (Smith & Pokorny, 1972). The firing rate MTF was derived as in Lee et al. (1990) and represents the contrast required to generate a 20 imp/s modulation in firing. Data with this arbitrary threshold measure are included to permit comparison with the earlier paper. The other curves represent the neurometric thresholds in the two conditions, with unknown or known phase. The solid curve represents psychophysical sensitivity at a similar retinal illuminance (2° field, 900 td) to the physiological measurements. It is replotted from Swanson et al. (1987), with cone contrast calculated using his stimulus wavelengths.

The firing rate MTF is similar to that in Lee et al. (1990); it shows some low-frequency roll-off and extends to 40–50 Hz. With the single-cell observer, the shape of the MTF becomes low pass. Knowledge of phase, which we suggest is equivalent to an observer knowing stimulus timing, improves sensitivity by a factor of 1.5–2.

Temporal sensitivity still extends to well beyond the 10- to 15-Hz psychophysical fusion limit. In terms of absolute sensitivity, the single-cell observer performs below the psychophysical level, unless phase is known. However, the shortfall in sensitivity is only by a factor of ~ 2 , which could be made up by a limited degree of summation over cells, as shown in later sections.

Figure 3B shows an equivalent analysis for PC cells and luminance modulation. Again, the firing rate curve resembles previous data (Lee et al., 1990). The neurometric curves are low pass. The psychophysical MTF is again replotted from Swanson et al. (1987). From the neurometric analysis, the sensitivity of PC cells approaches psychophysical sensitivity at very low temporal frequencies (<1 Hz), but the shape of the curves strongly diverges at higher frequencies.

Mean slope parameters for the fitted Weibull function are also summarized in Figure 3 for chromatic modulation; for luminance modulation, slopes were similar, but sometimes not well constrained because even at 100% contrast, 100% detection did not occur. As in Tolhurst et al. (1983), slope parameters generally ranged between 1.5 and 2.5 but decreased at higher temporal frequencies. This is a consequence of impulse statistics and was more marked with MC cells, as discussed below.

We performed a similar analysis for MC cells and luminance modulation. At higher frequencies, the effect of the discrete nature of impulse trains becomes marked. This is illustrated (for 19.5 Hz modulation) in Figure 4. For an unmodulated field (0% contrast), with a maintained firing of ~ 10 imp/s, about half the cycles contain zero impulses, most contain one impulse and a few contain more. Thus, most of the individual cycle first-harmonic amplitudes are either zero or distributed on a circle around the origin when there is just one impulse at a random phase (Figure 4A). At 12.5% contrast, 0–3 impulses occur per cycle, and at 50% contrast, 1–4 impulses per cycle are evoked. If impulses do occur, they tend to be tightly phase locked to the stimulus that constrains the amplitude of the first-harmonic, as also seen in Figure 4A. Peristimulus response histograms are shown for each condition, which illustrate the tendency toward multiple peaks, with one phase-locked impulse per peak. This is marked at high contrast where three distinct peaks occur, each representing an impulse tightly locked to the stimulus. The resulting distributions of response amplitudes now tend to be restricted to peaks corresponding to 0, 1, 2... impulses per cycle (Figure 4B). This results in ROC curves made up primarily of straight-line segments (Figure 4C). Because the underlying distributions are multimodal, the resulting neurometric functions are no longer well fit by Weibull functions, as seen in Figure 4D. Because even at high contrasts occasional cycles fail to evoke an impulse, 100% detection is approached less rapidly, and the slope of the fitted function becomes shallower. Cortical mechanisms must be able to analyze input signals in the face of these noncontinuous distributions

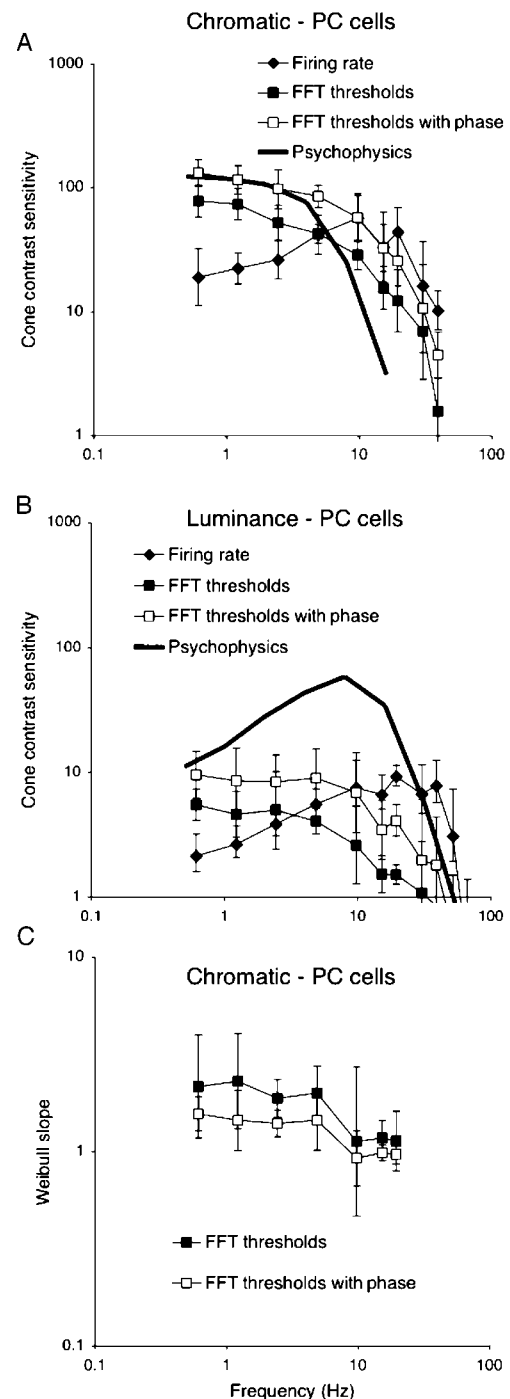


Figure 3. (A, B) Parvocellular (PC) cell and psychophysical sensitivity to chromatic and luminance modulation. Each point is the average of 5 cells (combined +M–L and +L–M). Sensitivity has been converted to cone contrast using the cone fundamentals. Thresholds derived for a 20 imp/s modulation in firing (firing rate) and two forms of neurometric analysis for a single-cell observer, either with unknown or known response phase, are shown. In this and subsequent figures, error bars indicate standard deviations of cell samples. Also shown are psychophysical thresholds for human observers from Swanson et al. (1987). (C) Mean slopes of Weibull function fits for the same cell sample. These values decrease at high temporal frequencies.

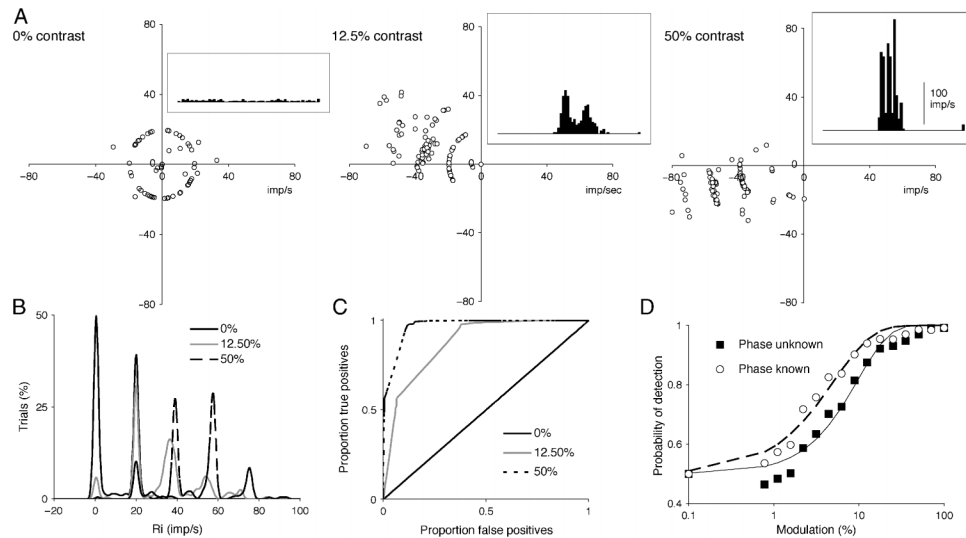


Figure 4. Distributions of Fourier coefficients of magnocellular (MC) cells at high frequency (luminance modulation, 19.5 Hz in illustration). (A) Results of single-cycle Fourier analysis at 0%, 12.5%, and 50% contrast. Inset histograms show averaged response. Because there are few impulses per cycle, individual points cluster around the circumference of circles representing 1, 2, 3, or 4 impulses per response, or at the origin (0 impulses per response). (B–C) Amplitude distributions were cumulated as in Figure 2. The quantal nature of the impulse distributions results in restricted values for the amplitude distributions, which leads to receiver operating characteristic (ROC) curves made up of combinations of straight-line segments. (D) Resulting frequency-of-detection functions tend to be of shallower slope due to the peculiar statistics of the distributions.

in the statistics of the input, although these effects tend to be washed out if many cells combine to input to detector mechanisms, as discussed in a later section.

We estimated neurometric thresholds for MC cells as a function of temporal frequency, and resulting curves (mean of five MC cells, on and off cells combined) are shown in Figure 5A. The firing rate curve resembles our previous report (Lee et al., 1990), with a peak at ~ 20 Hz and extending up to 60–70 Hz. The neurometric curves are also band-pass in shape, but with a peak frequency of 5–10 Hz. Fourier amplitude at, say, 40 Hz is high but signal-to-noise is low because of impulse statistical effects. Knowing response phase again improves sensitivity by a factor of 1.5–2. Psychophysical sensitivity (Swanson et al., 1987) peaks at an intermediate value (~ 10 Hz) and is greater than that of individual cells; 2° field, 900 td psychophysical data are shown. However, the shapes of the cellular and the psychophysical curves are similar, which supports our previous suggestion of the MC pathway as a substrate for detection of luminance flicker.

The noncontinuous nature of impulse distributions at high frequencies results in significant harmonic distortions of response histograms. Because the analysis in Figure 5 only used first-harmonic responses, this could result in reduced sensitivity. We therefore reanalyzed the data using a template-matching algorithm (Rüttiger, Lee, & Sun, 2002). This did not substantially improve sensitivity. Also, an advance in response phase with contrast is seen for the MC cell of Figure 4; this is not found in PC cells (Benardete, Kaplan, & Knight, 1992; Yeh, Lee, &

Kremers, 1995). However, the phase change involved was not large enough to substantially affect the analysis.

This analysis suggests that for luminance modulation and MC cells, a better match between physiology and psychophysics may be achieved by considering neural signal-to-noise ratios rather than peak firing rate. For MC cells and luminance modulation, the firing rate curve extends to 70–80 Hz, which is higher than the psychophysical CFF at this retinal illuminance. We originally proposed a central low-pass filter for this pathway, but the neurometric analysis reveals that the poor signal-to-noise ratio at high temporal frequencies may partly account for the difference. It is not necessary to postulate low-pass central filtering of the MC pathway signal. In the case of PC cells and chromatic modulation, the cellular MTF becomes low pass with neurometric analysis but still extends to 20–30 Hz, which is a higher frequency than the psychophysical chromatic CFF. Thus, central low-pass filtering of the PC pathway signal is still required. However, a more realistic model must also consider central detection mechanisms, to which we turn in the next section.

Central detection mechanisms

The neurometric analysis above was based on a sweep-by-sweep Fourier analysis, which implies detection mechanisms with time constants inversely proportional to frequency. This is clearly unrealistic. There have been suggestions (Hess & Snowden, 1992) of multiple temporal

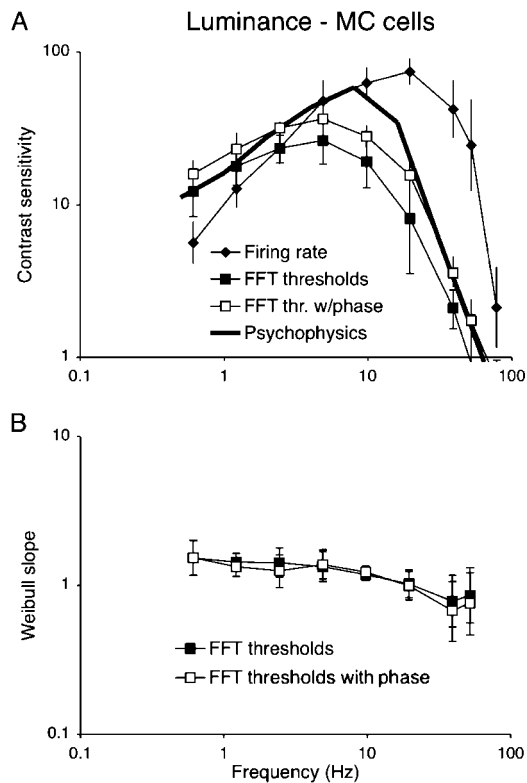


Figure 5. Temporal sensitivity of magnocellular (MC) cells to luminance modulation. (A) Comparison of MC cell temporal modulation transfer functions (MTFs). Mean of 7 cells, on and off cells combined. Shown are thresholds derived for a 20 imp/s modulation in firing (firing rate) and two forms of neurometric analysis for a single-cell observer, either with unknown or known response phase. Also shown are psychophysical thresholds for human observers from Swanson et al. (1987). (B) Mean slopes of Weibull function fits for the same cell fits for the same cell sample. These values decrease at high temporal frequencies.

channels in vision, but we assume here as a first step a detection mechanism with a fixed time constant operating at all frequencies.

Detection models considered in the psychophysical literature (e.g., Hood & Graham, 1998) often use a simple peak detector. This would compare the peak in some input waveform to a reference level. This may be unsatisfactory for handling neuronal spike trains because it needs to be referred to a baseline, maintained firing level. Such a detector might respond to drifts in mean firing rate, caused by, for example, level of arousal. Another drawback would be changes in mean signal as the mean firing rate (the zeroth harmonic) of the neuronal response increases with contrast. Even if a modulated response has been filtered out by, for example, a low-pass filter operating on the PC pathway, a DC response component will remain. We tested a simple peak detector and found this effect to be especially marked at high frequency.

A trough-to-peak detector is an alternative mechanism. As usually conceived, it would require a neural mecha-

nism to store the “trough” value while awaiting a “peak,” but it is not easy to see how this might be neuro-physiologically implemented. Another possible mechanism might be cell classes that respond in counterphase. In the case of chromatic modulation, these would be +L–M and +M–L cells and in the case of luminance modulation on- and off-center cells. A detector might look at the difference signal between such pathways, obviating the need to store a reference level. We tested such an approach on the impulse trains. Figure 6 shows the steps of the analysis, the example shown being a PC cell with chromatic modulation at 2.44 Hz.

The response to a cycle of modulation was converted from an impulse train to an analog signal by passing through an eight-stage filter with a 1-ms time constant. We have previously used this procedure on impulse trains for estimation of information content in responses to natural

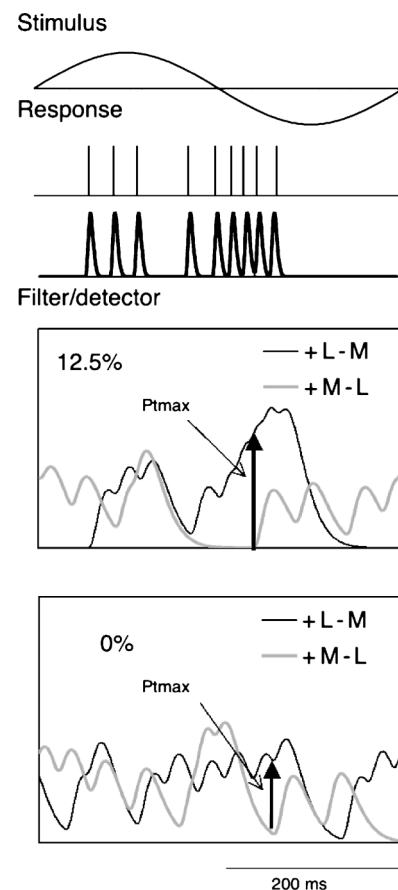


Figure 6. Sketch of implementation of peak detector comparing signals of +L–M and +M–L cells. The train of impulses in response to a sinusoidal stimulus (2.44 Hz) is converted into an analog signal by passing through an eight-stage filter with a time constant of 1 ms. This is subject to a filter/detector consisting of a three-stage filter with a time constant of 40 ms. The maximum difference signal between the two cells within a given cycle is ascertained and the resulting values is subject to neurometric analysis.

scenes (van Hateren, Rüttiger, Sun, & Lee, 2002). It is a means to provide for further analysis a convenient analog signal from a series of spike times, and the exact filter is not critical, provided its time constant is short. We then passed the converted analog impulse trains through a three-stage filter of a given time constant. This could be viewed as a detector or a filter preceding the detector. For each pair of cells, the output signals during each cycle were then compared and the maximum difference was identified, as indicated in Figure 6 for 12.5% and 0% contrast. The values Pt_{\max} for each cycle were then subject to the same form of neurometric analysis as in Figures 2 and 4.

Figure 7A shows results for PC cells and chromatic modulation with two detector time constants; the fast Fourier transform (FFT) threshold and psychophysical data have been replotted from Figure 3. With a 40-ms time constant, absolute sensitivity at low frequency is similar to the FFT analysis, but the high-frequency roll-off now parallels the psychophysical data. With a 10-ms time constant, the high-frequency response is enhanced at the cost of reduced sensitivity at low frequency. Figure 7B shows a similar analysis for PC cells and luminance modulation, which resulted in a similar remodeling of the FFT threshold curve. Figure 7C shows the analysis for MC cells with three different time constants. Increasing the filter/detector time constant decreases the high-frequency cutoff while improving low-frequency sensitivity. The best match in shape for the psychophysical data appears to be with a time constant of ~ 5 –10 ms, with neurometric sensitivity falling short of psychophysical sensitivity by about a factor of two.

It should be noted that comparing cells with opposite signs causes changes in mean rate (i.e., the zeroth harmonic) to cancel and thus not usable by a detection mechanism. The general validity of the Talbot–Plateau law suggests this is a reasonable approach.

Psychophysical temporal MTFs are directly related to critical duration tested with pulses of different length (Swanson et al., 1987). We tested if the filter/detector used for the MTFs provided an appropriate critical duration. Figure 8A shows examples of averaged responses of a +L–M and a +M–L cell to prolonged red chromatic pulses (1,500 ms duration, 12.5% diode contrast). The response is sustained. Such responses were recorded at a number of contrasts. Examples of impulse trains are shown in Figure 8B. Impulse trains associated with each response were analyzed using different window widths, as sketched, to mimic different pulse durations. These trains were passed through the same procedures as in Figure 6, that is, an initial filter to convert the pulse trains to an analog signal and a second filter and a detector. The difference signal between the two cells was subject to neurometric analysis as in previous sections.

Cell neurometric thresholds (in cone contrast, mean of 5 cell comparisons) are plotted as a function of pulse duration in Figure 8C. Thresholds decrease as pulse duration increases until they reach a plateau. We have

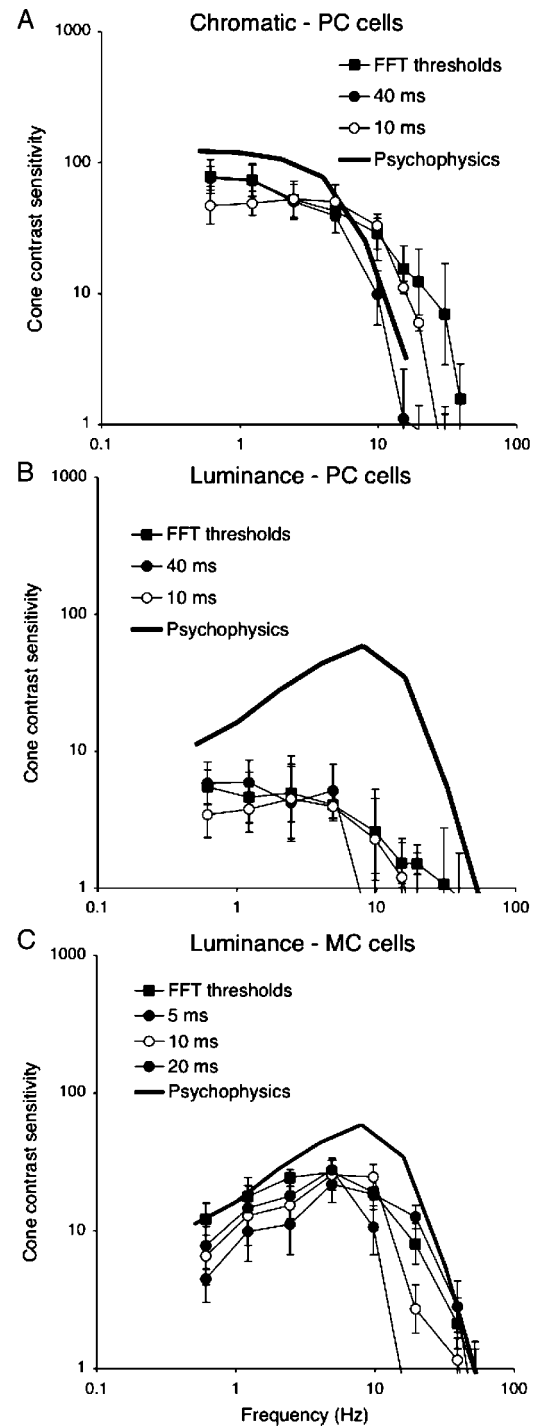


Figure 7. Temporal sensitivity of parvocellular (PC) cells to chromatic (A) and luminance (B) modulation and magnocellular (MC) cells to luminance modulation (C). Fast Fourier transform (FFT) thresholds and psychophysical data are replotted from Figures 3 and 5. For PC cells, detectors with time constants of 40 and 10 ms are shown; for MC cells, time constants of 5, 10, and 20 ms are shown. The best match of PC cells to psychophysical data is achieved with the 40-ms time constant. For MC cells, the 10-ms time constant gives the most satisfactory match.

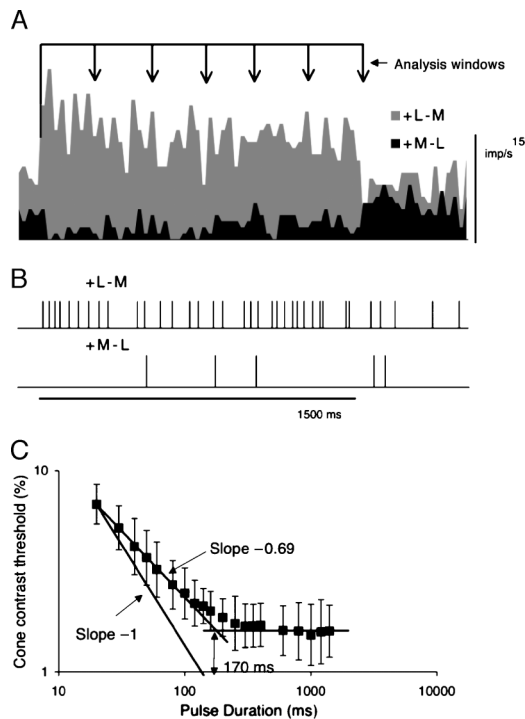


Figure 8. To test if the model detector gave appropriate critical durations, we recorded responses to long pulses and the model tested with different analysis windows. A response of +L–M and +M–L cell to 1,500-ms redward perturbations (mean of 30 responses, 12.5% diode modulation). (B) Examples impulse trains. These were converted to analog signals as in Figure 6 and were inserted into a filter as in that figure. For the different analysis windows, the signal was truncated and replaced by the maintained activity occurring after the 1,500-ms had elapsed. (C) Cone contrast thresholds of detector with 40 ms time constant as a function of pulse duration. Mean of five parvocellular (PC) cell pairs.

drawn straight lines through these sections, and they intersect at ~ 170 ms. This is consistent with critical duration estimates for chromatic pulses (Swanson et al., 1987). These authors' temporal summation curves were predictable from their psychophysical MTF data.

The finite impulse response of ganglion cells is not taken into account in the procedure above. For PC cells and chromatic modulation at the light level used here, the impulse response is monophasic with a width of 20–30 ms (Lee, Pokorny, Smith, & Kremers, 1994), which is short relative to that of the detector. As a control, we measured neurometric thresholds with a pulse duration of 100 ms, and the resulting values fell close to the curve in Figure 8.

These analyses are consistent with detection mechanisms with different time constants operating upon PC and MC signals to provide MTFs with shapes resembling those for psychophysical sensitivity. Three further features are of interest in Figure 8. Firstly, the absolute sensitivity levels in terms of cone contrast are similar for sinusoidal modulation (Figure 3) and for pulses. The plateau was reached at

$\sim 1.6\%$ cone contrast, which is similar to the low-frequency cone contrast sensitivity for sinusoidal modulation. Secondly, the slope of the descending limb of the relation in Figure 8 is less than one. This is probably because, for a single cell, as analysis duration increases, both signal strength (number of impulses in the response) and variability (variance in impulse number) are expected to increase. Impulse interval distributions of both MC and PC cells approximate low-order gamma distributions (Troy & Lee, 1994), at least for maintained activity. This might be expected to lead to an increase in signal-to-noise ratio with the square root of pulse duration, that is, a slope of -0.5 . The actual slope in Figure 8 is -0.69 . In psychophysical data such as those of Swanson et al. (1987), slopes are generally closer to minus one. The reason for this difference is uncertain. Lastly, over a critical duration of ~ 170 ms, just ~ 2 – 3 extra impulses are enough to enable a detector based on a single cell to detect a pulsed stimulus. This is close to the original estimate of detectability of ganglion cell responses proposed by Barlow and Levick (1969).

Summation of cell signals

An increase in psychophysical sensitivity over that of individual neurons might be achieved by probability summation (Watson, 1979) or by combination of cell inputs to a detector. The first of these was considered by Tolhurst et al. (1983); we here consider the second alternative. If signal and noise are additive, sensitivity of a detector should increase approximately as the square root of the number of inputs. We wished to test this by summing neuronal signals (up to 16) into the detection mechanism, but our physiological database did not contain enough cells. We therefore developed an algorithm to produce simulated neuronal responses (see Methods). For each cell type, responses of five cells were averaged and these were used as templates for the simulations. The resulting response histograms, interval distributions, and autocorrelograms closely resembled actual measurements.

Figures 9A and 9B show an analysis for PC cells and chromatic modulation. Convergence of 1, 2, 4, 8, and 16 cell pairs (i.e., difference signals of +M–L and +L–M cells) onto a central detector was simulated. Impulse trains were added, and the resulting waveform was subjected to neurometric analysis using a detector with a 40-ms time constant, as in the previous section. Figure 9A shows neurometric functions for different degrees of convergence for 0.61 Hz modulation. For clarity, only three (1, 4, and 16 cells) combinations are shown; the other levels (2 and 8 cells) fell in between. Sensitivity increased approximately with the square root of the number of cells providing input, for example, convergence of 4 cells provided a twofold increase in sensitivity. The fitted Weibull functions showed no systematic change of slope with convergence. Convergence did not change the shape of the MTF (Figure 9B). Psychophysical sensitivity could be matched by convergence of ~ 4 – 8 cells.

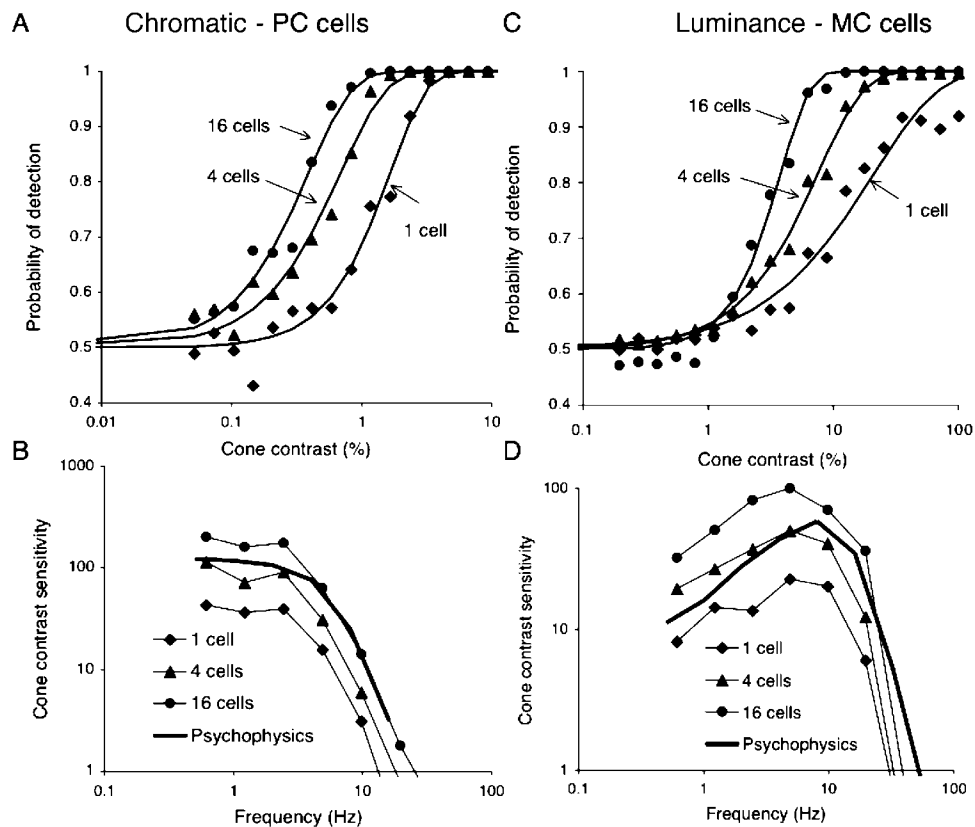


Figure 9. The effect of summation of cells before the detector. (A) Simulated parvocellular (PC) cell responses (2.44 Hz) were combined and subjected to neurometric analysis using the detector with a 40-ms time constant. The neurometric functions are shifted by combining cells which indicates an increase in sensitivity but there is little change in slope. (B) PC cell temporal sensitivity to chromatic modulation with different degrees of summation, together with psychophysical data replotted from earlier figures. (C) Simulated magnocellular (MC) cell responses (19.5 Hz) were combined and subjected to neurometric analysis using the detector with a 10-ms time constant. The neurometric functions are shifted by combining cells, which indicates an increase in sensitivity and an increase in slope. We attribute this to the increased number of impulses when cell signals are combined. (D) MC cell temporal sensitivity to luminance modulation with different degrees of summation, together with psychophysical data replotted from earlier figures.

This number should only be taken as a rough approximation because a central detection mechanism receiving inputs from a patch of retina seems unlikely to give all inputs equal weight. Figures 9C and 9D show an equivalent analysis for MC cells and luminance modulation. The probability of detection curves showed similar slopes at low frequency, but at higher frequency the increase in sensitivity with convergence was accompanied by a steepening of the Weibull function, as in the 19.5-Hz example in Figure 9C. This change is presumably a consequence of the increased number of impulses when inputs converge, resulting in a less marked effects arising from the impulse statistics shown in Figure 4. Sensitivity again increased approximately with the square root of the number of inputs, and the shape of the cellular MTF was little affected. Again, convergence of ~4–8 cells was required to match psychophysical sensitivity.

The results in this section indicate that sensitivity of a central detector increases with the square root of the number of inputs, and that only limited convergence would be required to attain psychophysical sensitivity.

This assumes that signals of neighboring ganglion cells are uncorrelated. It has been shown that some degree of synchrony may occur between cells in, for example, the salamander retina (Meister, Lagnado, & Baylor, 1995). In the primate, there have been shown to be correlations between the firing of MC cells (Shlens et al., 2006). The degree to which this correlation changes with contrast and affects detectability by a mechanism summing cells' signals is an important but unresolved question.

Cell convergence and the slope of the neurometric function

The slopes of neurometric functions for both ganglion and cortical cells range between 1.5 and 2.5, which is shallower than is typically observed on psychophysical tasks. Tolhurst et al. (1983) suggested that this discrepancy could be resolved by simultaneous triggering of several independent detectors, which then converge upon a further

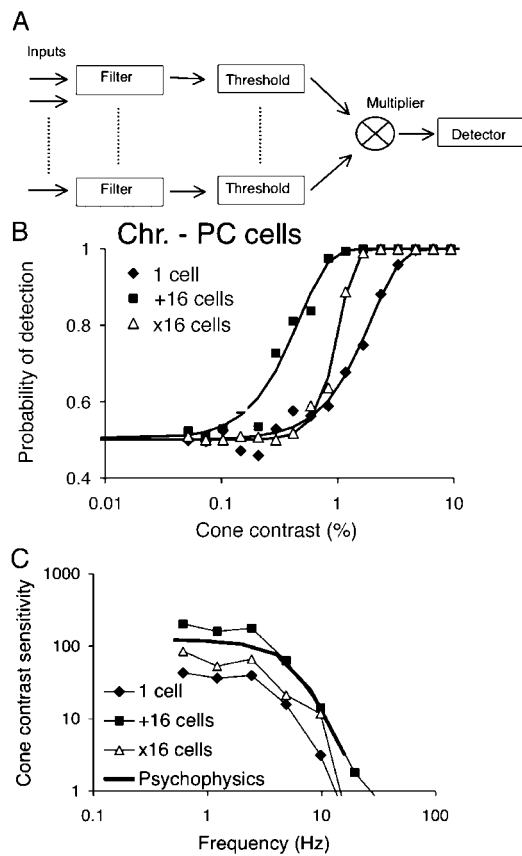


Figure 10. Possible scheme for increase in slope of fit of Weibull function to neurometric analysis. (A) Analog cell signals are filtered, subject to a thresholding mechanism and multiplied. The resulting output is subject to the differencing procedure described in previous figures. (B) Comparison of frequency of detection functions for a single cell, summed signals of 16 cells, and a combination of 16 cells used as input to the scheme in panel A, which increases slope. (C) PC temporal response to chromatic modulation for the three conditions compared to psychophysical data. The shapes of curves remain similar.

detector which requires their simultaneous activation to reach threshold (probability multiplication). We tested a more mechanistic implementation of this kind of model.

Figure 10A shows a schema of the approach. Each ganglion cell input is subject to filtering as described in previous sections, and the resulting signal is rectified by a thresholding mechanism. Resulting signals are multiplied and fed into the differential detector mechanism described above. We tested this model on sets of simulated impulse trains as in the previous section. Figure 10B shows an example of the effect of this operation on the steepness of neurometric functions, for a PC cell responding to chromatic modulation at 0.61 Hz. Data and fitted curves are shown for a single cell, and for additive convergence of 16 cells as described in the previous section. If input from 16 cells is provided to the multiplicative model, there is a steepening of the curve with an accompanying

loss of sensitivity. We applied this treatment to the same set of simulated PC cell spike trains as in the previous section, and averaged thresholds are compared with other conditions in Figure 10C. The shape of the temporal response curve is little affected, but there is a decrease in sensitivity by a factor of 2–3. Convergence from 16 cells provides thresholds approaching, but not reaching the psychophysical level. Neurometric slopes were increased at all temporal frequencies. On comparing the three conditions in Figure 10C in the frequency range from 0.61 to 4.88 Hz, neurometric slopes did not differ between the one cell and the additive 16-cell condition but significantly increased in the threshold/multiplicative condition. Over temporal frequencies from 0.61 to 9.8 Hz, mean fitted slope parameters were 2.19, 1.89, and 3.51 for a single cell, 16 cells added and 16 cells subjected to thresholding/multiplication, respectively. This was a highly significant difference (ANOVA, $F = 8.1$, $P < 1\%$).

Both elements in the model (thresholding and multiplicative interaction) sketched in Figure 10A are necessary; a threshold operation followed by additive combination of inputs did not steepen the function. The threshold level was set to be close to the maintained activity level. Lower thresholds caused little change in the neurometric function slope and higher thresholds provided very steep functions with severe loss of sensitivity.

The purpose of this simulation was to show that it is possible to steepen neurometric slopes by a nonlinear model other than the probability multiplication scheme of Tolhurst et al. (1983), but we would not suggest that the model in Figure 10 is the only or optimal alternative. However, steepening of the neurometric function and thresholds similar to those observed psychophysically would seem achievable with convergence from just a few cells; numerical estimates of the actual numbers of cells involved would require further assessment of spatial summation in central mechanisms.

Discussion

We have analyzed the temporal response of macaque ganglion cells to chromatic and luminance modulation through neurometric analysis of impulse trains (the single-cell observer), and then we consider possible central detection mechanisms. In an earlier description (Lee et al., 1990), the measure used was firing rate. When signal-to-noise ratio at different temporal frequencies is included in the analysis, this neurometric approach tends to produce an MTF shifted toward lower frequencies with less low-frequency attenuation in the MTF. However, for PC cells and chromatic modulation, central low-pass filtering of ganglion cell signals before detection was still required to provide an MTF similar to psychophysical measurements; alternatively the low-pass filtering could be a consequence

of a detector with long time constant. Contrary to our previous suggestion, no low-pass filtering was required to bring MC cell behavior in line with psychophysical measurements.

The results are consistent with the view that PC cells are responsible for the detection of chromatic modulation and MC cells for luminance modulation, except perhaps at low temporal frequencies (<2 Hz). We have found physiological properties and responsivities of PC and MC cell populations to be fairly homogenous. Of the multiple cell classes in the retina, MC and PC cells are the most numerous, and there is considerable ancillary evidence that they form the physiological substrate of psychophysical luminance and red–green chromatic channels, respectively (Lee, Martin, Valberg, & Kremers, 1993), and it seems likely that the role of other cell classes is minimal.

It has been suggested that multiple temporal mechanisms underlie detection of achromatic gratings. Hess and Snowden (1992) proposed that there are two or possibly three temporal mechanisms, one being low-pass and the other(s) band-pass. It is tempting to suppose that their low-pass mechanism might be based on the PC pathway because for luminance modulation this approached psychophysical sensitivity below 2–3 Hz. However, the temporal response of the Hess and Snowden low-pass mechanism extended up to 30 Hz. The PC pathway after low-pass filtering has a more limited frequency response. It remains feasible that the PC pathway supports detection of luminance modulation at low frequency; information rates for achromatic signals in the PC pathway exceeds those in the MC pathway below ~3 Hz (van Hateren et al., 2002).

Our physiological measurements were obtained from parafovea. We have compared them to foveal psychophysics (Swanson et al., 1987). In these and earlier experiments, we did not see any change of PC cell chromatic responsivity from 2° to 10° eccentricity. In another study (Martin, Lee, White, Solomon, & Rüttiger, 2001), PC cell chromatic responsivity was found to be maintained with little change to 20–40° eccentricity. For luminance flicker, we did not see any variation in cellular MTFs with eccentricity in the current experiments, although at high eccentricity CFF is increased (Solomon, Martin, White, Rüttiger, & Lee, 2002). Thus, a comparison between foveal psychophysics and parafoveal cell responsivities appears justified. The retinal illuminance in the psychophysical measurements of Swanson et al. (1987) was 900 td as compared to 2,000 td in our physiological measurements. These values are sufficiently close to make comparison valid because changes in the Swanson psychophysical data are most pronounced at lower retinal illuminances.

Central detection mechanisms

One goal of the current experiments was to constrain the properties of central detection mechanisms. These

have often been considered as peak detectors or trough-to-peak detectors. Both these alternatives require using a comparison reference level against which a possible signal may be measured. This could be mean firing rate, but it is difficult to see how this might be implemented in practice. Taking the difference signal between +L–M and +M–L PC cells for chromatic modulation, and between on- and off-center MC cells for luminance modulation, provides a plausible strategy for central detection mechanisms. Use of this difference signal avoids having to store reference values. This would not affect earlier conclusions as to the selective detection of positive- and negative-going ramps by the on and off pathways, respectively (Kremers, Lee, Pokorny, & Smith, 1993).

We have also considered how signals from numbers of cells may be combined either to enhance sensitivity or to steepen the slope of the neurometric function. With additive combination, sensitivity increases roughly as the square root of the number of input cells, as is the case for probability summation (Tolhurst et al., 1983). This is to be expected; adding cells together combines both their signals and their noise. Tolhurst et al. (1983) also suggested probability multiplication as a means of steepening neurometric function slope. They recognized that there is a consequent loss of sensitivity but suggested that this could be compensated by further neuronal summation. At a cortical level, there may be ample numbers of neurons for such manipulations, but the number of ganglion cells for a given retinal area is circumscribed. Furthermore, common noise in multiple inputs to detection mechanism severely degrades detectability (Zohary, Shadlen, & Newsome, 1994). This would occur if several central mechanisms shared inputs from individual members from a ganglion cell population. Thus, the probability multiplication approach is more complex than it appears at first sight.

In any event, the model in Figure 10 may be functionally equivalent to probability multiplication. The thresholding element of the model could be manifested in the progressive loss of maintained activity as one proceeds from retina into the cortex. For example, it appears that in the lateral geniculate nucleus, maintained firing is reduced compared to the retinal input, but most impulses evoked by a stimulus are transmitted to the cortex (Lee, Virsu, & Creutzfeldt, 1983). Multiplication or facilitation of neuronal signals in the cortex is well established (Alonso, Usrey, & Reid, 1996; Usrey, Alonso, & Reid, 2000). Some other features of a central analysis mechanism, which might result in a change of slope, have been discussed by Britten, Shadlen, Newsome, and Movshon (1992).

If the suggested detectors are present in the cortex, it is interesting to speculate how they might manifest themselves in cortical recordings. Recordings from V1 frequently show few cells that respond to low spatial frequencies or large targets, such as those used here. For luminance targets, cortical detectors may be linked to spatial contrast; for chromatic targets, this may be less

likely because psychophysical chromatic contrast sensitivity curves are low pass. One might seek appropriate cells in V1, but it is unclear whether this is the correct locus, or whether the properties suggested on the basis of these experiments should be sought in single cells or in cell assemblies.

Convergence and spatial extent

Both for PC cells and chromatic modulation, and MC cells and luminance modulation, input of only a restricted number of cells to a central detection mechanism appears necessary to reach psychophysical sensitivity levels. With simple cell summation or addition (Figure 9), combination of signals of very few cells (~ 4) is necessary to achieve psychophysical sensitivity. This is reminiscent of earlier analyses (Barlow, 1972; Barlow & Levick, 1969; Dhingra, Kao, Sterling, & Smith, 2003), in which it was proposed that signals for one or few ganglion cells are adequate for detection. This number would increase if some form of nonlinear mechanism as in Figure 10 increases the slope of the neurometric mechanism. Also, any correlation between neighboring cells of the same type might degrade the signal. In any event, the numbers of cells necessary would remain limited. How many cells are sufficient?

We used a 4.7° parafoveal stimulus, which, after M-scaling for retinal eccentricity (Virsu & Rovamo, 1979), would be equivalent to a foveal stimulus of $\sim 1.2^\circ$ in diameter. Foveal stimulus sizes used by Swanson et al. (1987) were 0.5° , 2° , and 8° . Psychophysical data for their two larger sizes were similar; there was reduced psychophysical sensitivity at high temporal frequencies (and a lower CFF) for the 0.5° field. For comparison with our physiology, we have plotted their 2° data. A more extensive description of area summation for luminance-modulated targets was provided by Mäkelä, Rovamo, and Whitaker (1994), who found that at 1 and 3 Hz Ricco's law held to a stimulus diameter of ~ 10 min, after which Piper's law applied until no further increase in sensitivity occurred above a diameter of ~ 40 min. It is possible that the Ricco's law slope primarily resulted from spatial summation within the ganglion cell receptive field center, whereas the shallower slope arose from summation of inputs to a central detector. However, at higher temporal frequencies, Mäkelä et al. found that sensitivity increased to larger target sizes. This may also have a physiological basis. We noted in preliminary observations that the temporal response of MC cells significantly depends on spot size; with a spot restricted to the center, low-frequency sensitivity is similar or slightly greater than that to large fields, but high-frequency sensitivity falls as does the CFF. This is likely to be due to temporal interactions arising from the center/surround latency difference; at high frequency, as a spot encroaches into the surround, responses are enhanced (Nadig, Lee, Smith, & Pokorny, 1995).

On the basis of counts of foveal parasol cell density (Grünert, Greferath, Boycott, & Wässle, 1993) and estimates of foveal parasol cell receptive field center size from the literature (Derrington & Lennie, 1984), we estimate that ~ 3 – 400 on-center (and a similar number of off-center) parasol cell centers would be completely covered by a 40 -min target. Again, based on receptive field dimensions from the literature (Croner & Kaplan, 1995; Lee, Kremers, & Yeh, 1998), ~ 2 times this number of +L–M on-center cells' receptive fields would be covered despite the greater density of this cell type; for an L,M-cone opponent cell to respond maximally to red–green chromatic modulation, both center and surround have to be completely covered by the spot because both contribute to the response. Unfortunately, psychophysical data describing red–green chromatic sensitivity to modulated targets as a function of target size are unavailable.

Additional psychophysical and physiological data obtained with different targets may permit construction of an adequate model incorporating spatial parameters. A further factor is whether, with a large spot, cells or detectors near its edge determine psychophysical threshold. Modulation sensitivity of observers is greatly enhanced by setting the stimulus in a surround of the same mean luminance rather than on a dark background, at least at low temporal frequencies (Spehar & Zaidi, 1997), perhaps due to the action of local contrast detectors. If detectors close to the edge of a flickering field determine detection, this would also be also be relevant to cell convergence in a spatial model.

Acknowledgments

We would like to thank Paul Martin, Joel Pokorny, Bill Swanson, and Arne Valberg for discussion and comments on the manuscript. This work was supported by NIH EY 13112 to BBL.

Commercial relationships: none.

Corresponding author: Barry B. Lee.

Email: blee@sunopt.edu.

Address: Suny College of Optometry, 33 W42nd St., NY, NY 10036, USA.

References

- Alonso, J. M., Usrey, W. M., & Reid, R. C. (1996). Precisely correlated firing in cells of the lateral geniculate nucleus. *Nature*, *383*, 815–819. [PubMed]
- Barlow, H. B. (1972). Single units and sensation: A neuron doctrine for perceptual psychology? *Perception*, *1*, 371–394. [PubMed]

- Barlow, H. B., & Levick, W. R. (1969). Three factors limiting the reliable detection of light by retinal ganglion cells of the cat. *The Journal of Physiology*, *200*, 1–24. [[PubMed](#)] [[Article](#)]
- Benardete, E. A., Kaplan, E., & Knight, B. W. (1992). Contrast gain control in the primate retina: P cells are not X-like, some M cells are. *Visual Neuroscience*, *8*, 483–486. [[PubMed](#)]
- Britten, K. H., Newsome, W. T., Shadlen, M. N., Celebrini, S., & Movshon, J. A. (1996). A relationship between behavioral choice and the visual responses of neurons in macaque MT. *Visual Neuroscience*, *13*, 87–100. [[PubMed](#)]
- Britten, K. H., Shadlen, M. N., Newsome, W. T., & Movshon, J. A. (1992). The analysis of visual motion: A comparison of neural and psychophysical performance. *Journal of Neuroscience*, *12*, 4745–4765. [[PubMed](#)] [[Article](#)]
- Croner, L. J., & Kaplan, E. (1995). Receptive fields of P and M ganglion cells across the primate retina. *Vision Research*, *35*, 7–24. [[PubMed](#)]
- Croner, L. J., Purpura, K., & Kaplan, E. (1993). Response variability in retinal ganglion cells of primates. *Proceedings of the National Academy of Sciences of the United States of America*, *90*, 8128–8130. [[PubMed](#)] [[Article](#)]
- Crook, J. M., Lange-Malecki, B., Lee, B. B., & Valberg, A. (1988). Visual resolution of macaque retinal ganglion cells. *The Journal of Physiology*, *396*, 205–224. [[PubMed](#)] [[Article](#)]
- Derrington, A. M., & Lennie, P. (1984). Spatial and temporal contrast sensitivities of neurones in lateral geniculate nucleus of macaque. *The Journal of Physiology*, *357*, 219–240. [[PubMed](#)] [[Article](#)]
- Dhingra, N. K., Kao, Y. H., Sterling, P., & Smith, R. G. (2003). Contrast threshold of a brink-transient ganglion cell in vitro. *Journal of Neurophysiology*, *89*, 2360–2369. [[PubMed](#)] [[Article](#)]
- Grünert, U., Greferath, U., Boycott, B. B., & Wässle, H. (1993). Parasol (P α) ganglion cells of the primate fovea: Immunocytochemical staining with antibodies against GABAA-receptors. *Vision Research*, *33*, 1–14. [[PubMed](#)]
- Hess, R. F., & Snowden, R. J. (1992). Temporal properties of human visual filters: Number, shapes and spatial covariation. *Vision Research*, *32*, 47–59. [[PubMed](#)]
- Hood, D. C., & Graham, N. (1998). Threshold fluctuations on temporally modulated backgrounds: A possible physiological explanation based upon a recent computational model. *Visual Neuroscience*, *15*, 957–968. [[PubMed](#)]
- Kremers, J., Lee, B. B., Pokorny, J., & Smith, V. C. (1993). Responses of macaque ganglion cells and human observers to compound periodic waveforms. *Vision Research*, *33*, 1997–2011. [[PubMed](#)]
- Lee, B. B., Kremers, J., & Yeh, T. (1998). Receptive fields of primate retinal ganglion cells studied with a novel technique. *Visual Neuroscience*, *15*, 161–175. [[PubMed](#)]
- Lee, B. B., Martin, P. R., & Valberg, A. (1989). Sensitivity of macaque retinal ganglion cells to chromatic and luminance flicker. *The Journal of Physiology*, *414*, 223–243. [[PubMed](#)] [[Article](#)]
- Lee, B. B., Martin, P. R., Valberg, A., & Kremers, J. (1993). Physiological mechanisms underlying psychophysical sensitivity to combined luminance and chromatic luminance modulation. *Journal of the Optical Society of America A, Optics and image science*, *10*, 1403–1412. [[PubMed](#)]
- Lee, B. B., Pokorny, J., Smith, V. C., & Kremers, J. (1994). Responses to pulses and sinusoids in macaque ganglion cells. *Vision Research*, *34*, 3081–3096. [[PubMed](#)]
- Lee, B. B., Pokorny, J., Smith, V. C., Martin, P. R., & Valberg, A. (1990). Luminance and chromatic modulation sensitivity of macaque ganglion cells and human observers. *Journal of the Optical Society of America A, Optics and image science*, *7*, 2223–2236. [[PubMed](#)]
- Lee, B. B., Virsu, V., & Creutzfeldt, O. D. (1983). Linear signal transmission from prepotentials to cells in the macaque lateral geniculate nucleus. *Experimental Brain Research*, *52*, 50–56. [[PubMed](#)]
- Lee, B. B., Wehrhahn, C., Westheimer, G., & Kremers, J. (1993). Macaque ganglion cell responses to stimuli that elicit hyperacuity in man: Detection of small displacements. *Journal of Neuroscience*, *13*, 1001–1009. [[PubMed](#)] [[Article](#)]
- Mäkelä, P., Rovamo, J., & Whitaker, D. (1994). Effects of luminance and early temporal noise on flicker sensitivity as a function of stimulus size at various eccentricities. *Vision Research*, *34*, 1981–1991. [[PubMed](#)]
- Martin, P. R., Lee, B. B., White, A. J., Solomon, S. G., & Rüttiger, L. (2001). Chromatic sensitivity of ganglion cells in the peripheral primate retina. *Nature*, *410*, 933–936. [[PubMed](#)]
- Meister, M., Lagnado, L., & Baylor, D. A. (1995). Concerted signaling by retinal ganglion cells. *Science*, *270*, 1207–1210. [[PubMed](#)]
- Nadig, M., Lee, B. B., Smith, V. C., & Pokorny, J. (1995). Model of temporal processing in macaque retinal ganglion cells. *Investigative Ophthalmology & Visual Science*, *36*, S931.
- Naka, K. I., & Rushton, W. A. (1966). S-potentials from colour units in the retina of fish (Cyprinidae). *The Journal of Physiology*, *185*, 536–555. [[PubMed](#)] [[Article](#)]

- Pokorny, J., Smithson, H., & Quinlan, J. (2004). Photostimulator allowing independent control of rods and the three cone types. *Visual Neuroscience*, *21*, 263–267. [[PubMed](#)]
- Rüttiger, L., Lee, B. B., & Sun, H. (2002). Transient cells can be neurometrically sustained; the positional accuracy of retinal signals to moving targets. *Journal of Vision*, *2*(3):3, 232–242, <http://journalofvision.org/2/3/3/>, doi:10.1167/2.3.3. [[PubMed](#)] [[Article](#)]
- Shlens, J., Field, G. D., Gauthier, J. L., Grivich, M. I., Petrusca, D., Sher, A., et al. (2006). The structure of multi-neuron firing patterns in primate retina. *Journal of Neuroscience*, *26*, 8254–8266. [[PubMed](#)] [[Article](#)]
- Smith, V. C., Lee, B. B., Pokorny, J., Martin, P. R., & Valberg, A. (1992). Responses of macaque ganglion cells to the relative phase of heterochromatically modulated lights. *The Journal of Physiology*, *458*, 191–221. [[PubMed](#)] [[Article](#)]
- Smith, V. C., & Pokorny, J. (1972). Spectral sensitivity of color-blind observers and the human cone photopigments. *Vision Research*, *12*, 2059. [[PubMed](#)]
- Solomon, S. G., Martin, P. R., White, A. J., Rüttiger, L., & Lee, B. B. (2002). Modulation sensitivity of ganglion cells in peripheral retina of macaque. *Vision Research*, *42*, 2893–2898. [[PubMed](#)]
- Spehar, B., & Zaidi, Q. (1997). Surround effects on the shape of the temporal contrast-sensitivity function. *Journal of Optical Society of America A, Optics, image science, and vision*, *14*, 2517–2525. [[PubMed](#)]
- Sun, H., Rüttiger, L., & Lee, B. B. (2004). The spatiotemporal precision of ganglion cell signals: A comparison of physiological and psychophysical performance with moving gratings. *Vision Research*, *44*, 19–33. [[PubMed](#)]
- Swanson, W. H., Ueno, T., Smith, V. C., & Pokorny, J. (1987). Temporal modulation sensitivity and pulse detection thresholds for chromatic and luminance perturbations. *Journal of the Optical Society of America A, Optics and image science*, *4*, 1992–2005. [[PubMed](#)]
- Teich, M. C., Matin, L., & Cantor, B. I. (1978). Refractoriness in the maintained discharge of the cat's retinal ganglion cell. *Journal of the Optical Society of America*, *68*, 386–401. [[PubMed](#)]
- Tolhurst, D. J., Movshon, J. A., & Dean, F. A. (1983). The statistical reliability of signals in single neurons in cat and monkey visual cortex. *Vision Research*, *23*, 775–785. [[PubMed](#)]
- Troy, J. B., & Lee, B. B. (1994). Steady discharges of macaque retinal ganglion cells. *Visual Neuroscience*, *11*, 111–118. [[PubMed](#)]
- Usrey, W. M., Alonso, J. M., & Reid, R. C. (2000). Synaptic interactions between thalamic inputs to simple cells in cat visual cortex. *Journal of Neuroscience*, *20*, 5461–5467. [[PubMed](#)] [[Article](#)]
- van Hateren, J. H., Rüttiger, L., Sun, H., & Lee, B. B. (2002). Processing of natural temporal stimuli by macaque retinal ganglion cells. *Journal of Neuroscience*, *22*, 9945–9960. [[PubMed](#)] [[Article](#)]
- Virsu, V., & Lee, B. B. (1983). Light adaptation in cells of macaque lateral geniculate nucleus and its relation to human light adaptation. *Journal of Neurophysiology*, *50*, 864–877. [[PubMed](#)]
- Virsu, V., & Rovamo, J. (1979). Visual resolution, contrast sensitivity, and the cortical magnification factor. *Experimental Brain Research*, *37*, 475–494. [[PubMed](#)]
- Watson, A. B. (1979). Probability summation over time. *Vision Research*, *19*, 515–522. [[PubMed](#)]
- Westheimer, G. (1966). The Maxwellian view. *Vision Research*, *6*, 669–682. [[PubMed](#)]
- Yeh, T., Lee, B. B., & Kremers, J. (1995). The temporal response of ganglion cells of the macaque retina to cone-specific modulation. *Journal of the Optical Society of America A, Optics, image science, and vision*, *12*, 456–464. [[PubMed](#)]
- Zohary, E., Shadlen, M. N., & Newsome, W. T. (1994). Correlated neuronal discharge rate and its implications for psychophysical performance. *Nature*, *370*, 140–143. [[PubMed](#)]